Application Note

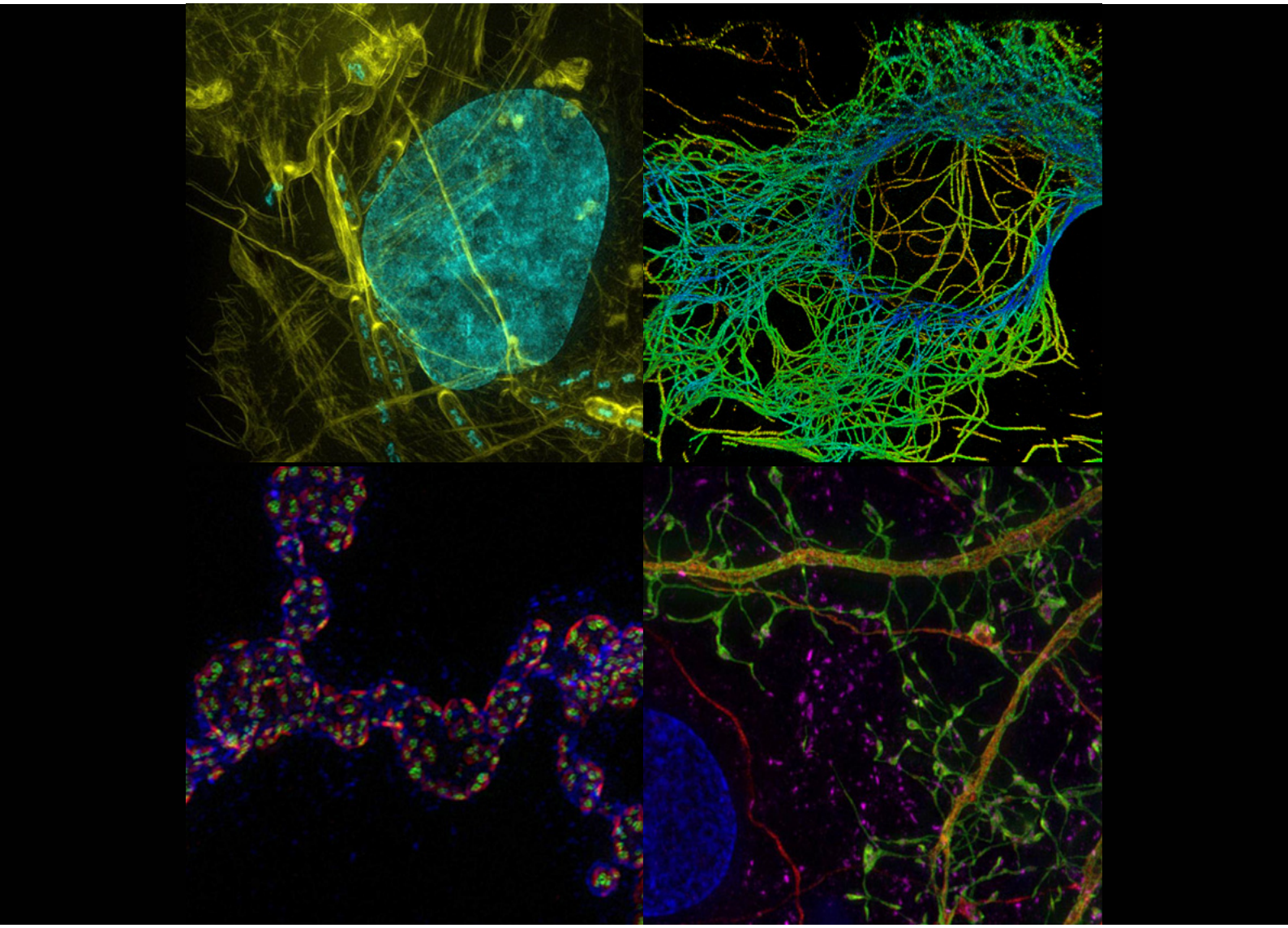

ZEISS Elyra PS.1

Imaging Biological Samples – a Reference List

ZEISS ELYRA PS.1

Imaging Biological Samples – a Reference List

Authors: Dr. Renée Dalrymple, Dr. Klaus Weisshart
Dr. Rebecca Elsaesser, Dr. Christian Hellriegel
Carl Zeiss Microscopy GmbH, Germany

Date: November 2017

Introduction

Superresolution light microscopy methods have opened doors to the observation of structures beyond the diffraction limit of light. Two of the methods which have been widely used are Superresolution Structured Illumination microscopy (SR-SIM) and photoactivated localization microscopy (PALM). SR-SIM uses the interaction of a patterned illumination source with the fluorescence in the sample to extract higher frequency information. The pattern is shifted across the image at several angles and the resulting information is reconstructed to form an image with up to a two fold increase in resolution in all three dimensions. In PALM, the locations of individual fluorescent probes are determined in order to generate a high precision map of the sample with approximately a ten fold improvement in resolution over the diffraction limit. This provides researchers with the highest resolution fluorescence microscopy images possible today.

Elyra PS.1 provides both of these superresolution techniques, which have been used by numerous scientists to advance their research. The two fold improvement in resolution afforded by SR-SIM is easily achieved in a variety of samples as it does not require specialized fluorescent probes; therefore, up to four fluorescent channels can be easily acquired. Multiple grids ensure the patterned illumination and thus resolution is optimized for each fluorescent channel and the ability to select three or five rotations provides nearly isotropic images. SR-SIM with Elyra S.1 offers a convenient superresolution technique that has been widely used to study cellular machinery previously unresolvable with fluorescent microscopy.

For those applications requiring an even higher level of resolution, Elyra PS.1 also provides capabilities for PALM. Here, 3D localization is determined by the unique method of double phase ramp imaging localization microscopy based on the technique PRILM, pioneered by David Baddeley at Yale University [4]. This provides the largest axial capture range among 3D localization techniques, 1.4 µm, as well as a localization precision that is independent of the axial position. Researchers have used this capability to determine the subcellular location of numerous proteins as well as studying their proximity to one another. Additionally, superresolution light microscopy techniques can be combined with electron microscopy through correlative light and electron microscopy (CLEM) to provide further insights into cell biology [5].
This reference list compiles many scientific works that have utilized the unique capabilities of Elyra to benefit from the superresolution techniques SR-SIM and PALM.

Localization Microscopy

Publication	Sample	Application
Yang, W., et al., (2014). Antioxidant Signaling Involving the Microtubule Motor KIF12 Is an Intracellular Target of Nutrition Excess in Beta Cells, Developmental Cell, Volume 31, Issue 2, 27 October 2014, Pages 202-214, ISSN 1534-5807, doi:10.1016/j.devcel.2014.08.028	WT and KIF12 knockout mice, mCitrine-KIF12-expressing KO primary beta cells	Colocalization of Sp1/KIF12/a-tubulin and Sp1/KIF12/Hsc70 using three color PALM/dSTORM. Fluorophores: mCitrine, Alexa Fluor® 568, Alexa Fluor® 647
Bach, J. N., et al., (2017). Sample Preparation and Choice of Fluorophores for Single and Dual Color Photo-Activated Localization Microscopy (PALM) with Bacterial Cells. Light Microscopy: Methods and Protocols, 129 -141. Springer New York, NY. doi:10.1007/978-1-4939-6810-7_9	Bacteria	Preparation of bacterial samples for PALM using fluorophores such as mNeonGreen, Dendra2, and PAm-Cherry. Multicolor PALM and TIRF
Reuss, M., et al., (2017). Measuring true localization accuracy in super resolution microscopy with DNA-origami nanostructures, New Journal of Physics, vol 19, 2, 025013, 2017, doi:10.1088/1367-2630/aa5f74	DNA-origami nanorods and CAGE 552-modified oligonucleotides	Assesement of localization accuracy of STED and STORM.
Kasula, R., et al., (2016). The Munc18-1 domain 3a hinge-loop controls syntaxin-1A nanodomain assembly and engagement with the SNARE complex during secretory vesicle priming. J Cell Biol Sep 2016, 214 (7) 847-858; doi:10.1083/jcb.201508118	DKD-PC12 cells transfected with Munc18-1-mEos2 or Munc18-1Δ317-333-mEos2, syntaxin-1A Alexa Fluor 647	sptPALM, uPAINT, correlative light and electron microscopy
Yejun, W., et al., (2017). Superresolution imaging of nanoscale chromosome contacts. Sci. Rep. 7, 42422; doi:10.1038/srep42422	chromatin spreads	BALM imaging with YOYO-1, three color superresolution imaging
Liang, H., et al., (2017). Metabolic labelling of the carbohydrate core in bacterial peptidoglycan and its applications. Nature Communications, 8:15015, 2017, doi:10.1038/ncomms15015	Bacteria (E. coli and P. putida)	SIM and 3D localization microscopy of N-acetyl-muramic acid backbone of bacterial peptidoglycan labeled with click chemistry
Liebmann, T., et al., (2013). Nanoscale elucidation of Na,K-ATPase isoforms in dendritic spines. Optical Nanoscopy 2013 2:6, doi:10.1186/2192-2853-2-6	cultured neurons	Photoactivated Localization Microscopy (PALM) imaging for investigation of the membrane bound sodium pump, Na,K-ATPase
Mohr, M. A., et al., (2017). Rational Engineering of Photoconvertible Fluorescent Proteins for Dual-Color Fluorescence Nanoscopy Enabled by a Triplet-State Mechanism of Primed Conversion. Angew. Chem. doi:10.1002/ange.201706121	Photoconvertable fluorescent protein development	Development of primed varients of green-to-red photoconvertible fluorescent proteins.
Miklosi, A. G., et al., (2017). Super-resolution Microscopical Localization of Dopamine Receptors 1 and 2 in Rat Hippocampal Synaptosomes. Molecular Neurobiology 2017, doi:10.1007/s12035-017-0688-y	isolated synaptosomes from rat hippocampi	dSTORM of dopamine receptors D1 and D2
Mollazade, M., et al., (2017). Can single molecule localization microscopy be used to map closely spaced RGD nanodomains? PLoS ONE 12(7): e0180871. 2017, doi:10.1371/journal.pone.0180871	cell adhesion-stimulating tripeptide arginine-glycine-aspartic acid (RGD) on nanopatterned surfaces	dSTORM and spatial cluster analysis to detect nanodomains of ligands on nanopatterned surfaces
Young C. L., et al., (2012). Cassette series designed for live-cell imaging of proteins and high-resolution techniques in yeast. Yeast 29 (2-3): 119-136. Epub 2012 Apr 4 2012. doi:10.1002/yea.2895	yeast (S. cerevisiae)	cassette design for high-resolution techniques in yeast, PALM imaging of Sec61mEos2 fusion proteins in S. cerevisiae
Noda, Y., et al., (2012). Phosphatidylinositol 4-phosphate 5-kinase alpha (PIPKα) regulates neuronal microtubule depolymerase kinesin, KIF2A and suppresses elongation of axon branches. PNAS 2012 109 (5) 1725-1730; published ahead of print January 17, 2012, doi:10.1073/pnas.1107808109	cultured developing hippocampal neurons	PALM imaging of KIF2A and PIPKα in growth cones
Nakata, T., et al., (2011). Preferential binding of a kinesin-1 motor to GTP-tubulin–rich microtubules underlies polarized vesicle transport. The Journal of Cell Biology Jul 2011, 194 (2) 245-255; doi:10.1083/jcb.201104034	stage 4 hippocampal neurons	Localization microscopy of GTP-tubulin clusters and KIF5 binding sites
Abe M., et al., (2012). A Role for Sphingomyelin-Rich Lipid Domains in the Accumulation of Phosphatidylinositol-4,5-Bisphosphate to the Cleavage Furrow during Cytokinesis. Mol. Cell. Biol. April 2012 vol. 32 no. 8 1396-1407, doi:10.1128/MCB.06113-11	LLC-PK1 cells	PALM/dSTORM imaging of transbilayer colocalization of sphingomyelin rich domains in the outer leaflet and PIP2-rich domains in the inner leaflet of plasma membrane
Owen, D. M., et al., (2010). PALM imaging and cluster analysis of protein heterogeneity at the cell surface. J Biophotonics. 2010 Jul;3(7):446-54. doi:10.1002/jbio.200900089	T cells	PALM and dSTORM imaging of protein distribution on the plasma membrane

Single Particle Tracking

Publication	Sample	Application
Yang, W., et al., (2014). Antioxidant Signaling Involving the Microtubule Motor KIF12 Is an Intracellular Target of Nutrition Excess in Beta Cells, Developmental Cell, Volume 31, Issue 2, 27 October 2014, Pages 202-214, ISSN 1534-5807, doi:10.1016/j.devcel.2014.08.028	WT and KIF12 knockout mice, mCitrine-KIF12-expressing KO primary beta cells	Colocalization of Sp1/KIF12/a-tubulin and Sp1/KIF12/Hsc70 using three color PALM/dSTORM. Fluorophores: mCitrine, Alexa Fluor® 568, Alexa Fluor® 647

Superresolution Structured Illumination Microscopy

Publication	Sample	Application
Nozumi, M., et al., (2017). Co+A24:C54rdinated Movement of Vesicles and Actin Bundles during Nerve Growth Revealed by Superresolution Microscopy. Cell Reports Feb 2017, doi:10.1016/j.celrep.2017.02.008	growth cones, mouse cortical neurons	Live-cell SIM of vesicular proteins, endocytosis related proteins, Gpm6a and the cholesterol probe GFP-D4
Minegishi et al., (2017). A Wnt5 Activity Asymmetry and Intercellular Signaling via PCP Proteins Polarize Node Cells for Left-Right Symmetry Breaking, Elsevier Inc. March 2017, Developmental Cell 40, 439–452, doi:10.1016/j.devcel.2017.02.010	sagittal sections (4 mm thick) from immunostained node samples	SIM imaging to determine the subcellular localization of Vangl1, Prickle2, and Vangl2 in node cells of the embryo
Ngo, A. T. P., et al., (2017). Assessment of roles for the Rho-specific guanine nucleotide dissociation inhibitor (RhoGDI) Ly-GDI in platelet function: a spatial systems approach. Articles in Press. Am J Physiol Cell Physiol (February 1, 2017). doi:10.1152/ajpcell.00274.2016	platelets	SR-SIM imaging of adherent platelets, two-channel colocalization
Fischer et al., (2017). Chlamydia trachomatis-containing vacuole serves as eubiquitination platform to stabilize Mcl-1 and to interfere with host defense. eLife 2017;6:e21465. doi:10.7554/eLife.21465	HeLa229 and HEp-2 cells infected with C. trachomatisstrains	SR-SIM imaging to determine Mcl-1-ubiquitin co-localization
Lekholm E., et al., (2017). Putative Membrane-Bound Transporters MFSD14A and MFSD14B Are Neuronal and Affected by Nutrient Availability. Front. Mol. Neurosci. 10:11. doi:10.3389/fnmol.2017.00011	primary mouse embryonic cortex cultures from embryos at day 14-16	"Subcellular localization of orphan transporters MFSD14A and MFSD14B using SR-SIM"
Burnette, D. T., et al., (2014). A contractile and counterbalancing adhesion system controls the 3D shape of crawling cells. J. Cell Biol. Vol. 205 No. 1 83–96. doi:10.1083/jcb.201311104	Fixed cells mounted in Vectashield H-1000 (Vector Laboratories). U2OS cells, primary MEF cells	SR-SIM of actin filaments, myosin IIA, and paxillin
Reintjes, G., et al., (2017). An alternative polysaccharide uptake mechanism of marine bacteria. The ISME Journal advance online publication, 21 March 2017. doi:10.1038/ismej.2017.26	microbial communities from the Atlantic ocean	SR-SIM imaging to determine polysaccharide hydrolysis by microbial communities
Chowdhury, S. R., et al., (2017). Chlamydia preserves the mitochondrial network necessary for replication via microRNA-dependent inhibition of fission. J. Cell Biol. doi:10.1083/jcb.201608063	HUVECs infected with C. trachomatis	SR-SIM imaging of HUVECs infected with C. trachomati and Drp1 fission rings in mitochondria
Qu, Y., et al., (2017). Periodic actin structures in neuronal axons are required to maintain microtubules. Mol. Biol. Cell January 15, 2017 vol. 28 no. 2 296-308, doi:10.1091/mbc.E16-10-0727	primary Drosophila neuronal axons	Periodic membrane skeleton abundance, organization and function
Absalon, S., et al., (2016). An essential malaria protein defines the architecture of blood-stage and transmission-stage parasites. Nature Communications, 7:11449, doi:10.1038/ncomms11449	P. falciparum parasites mounted in Vectashield	replication and maturation of malaria parasites
Trivedi, N., et al., (2017). Drebrin-mediated microtubule–actomyosin coupling steers cerebellar granule neuron nucleokinesis and migration pathway selection. Nature Communications, 8:14484, doi:10.1038/ncomms14484	cerebellar granule neuron cultures	Live and fixed cell SR-SIM and Lattice light-sheet imaging of the proximal leading process nanoscale architecture
Kahr, W. H. A., et al., (2017). Loss of the Arp2/3 complex component ARPC1B causes platelet abnormalities and predisposes to inflammatory disease. Nature Communications, 8: 14816, doi:10.1038/ncomms14816	platelets	SR-SIM imaging of CD61/fibrinogen receptor, ARPC5 and F-actin in platelets
Grangeon, R., et al., (2015). PopZ identifies the new pole, and PodJ identifies the old pole during polar growth in Agrobacterium tumefaciens. PNAS 2015 112 (37) 11666-11671; published ahead of print August 31, 2015, doi:10.1073/pnas.1515544112	Rod shaped bacteria, plant pathogen Agrobacterium tumefaciens	Examination of bacterial unipolar growth by imaging PopZAt-GFP and RFP-PodJAt by 3D-SIM
Marwaha, R., et al., (2017). The Rab7 effector PLE KHM1 binds Arl8b to promote cargo traffic to lysosomes. J Cell Biol Apr 2017, 216 (4) 1051-1070; doi:10.1083/jcb.201607085	Cultured cells	SR-SIM imaging of small GTPases, such as Rab7 and Arl8b
Sharif, M., et al., (2017). Redistribution of soluble N-ethylmaleimide-sensitive-factor attachment protein receptors in mouse sperm membranes prior to the acrosome reaction. Biology of Reproduction, 2017, 96(2), 352–365, doi:10.1095/biolreprod.116.143735	mouse sperm	SR-SIM imaging of syntaxin 2, VAMP2, ZP3R

Superresolution Structured Illumination Microscopy (cont.)

Publication	Sample	Application
Traver, M. K., et al., (2017). T Cell Receptor Activation of NF-κB in Effector T Cells: Visualizing Signaling Events Within and Beyond the Cytoplasmic Domain of the Immunological Synapse. Baldari. C. T., et al., The Immune Synapse: Methods and Protocols, Methods in Molecular Biology, vol. 1584, doi:10.1007/978-1-4939-6881-7_8	D10 murine T cells	SR-SIM imaging of Bcl10-CFP and Malt1-YFP
Singh, P., et al., (2014). Single-vesicle architecture of synaptobrevin2 in astrocytes. Nature Communications, 5:3780, doi:10.1038/ncomms4780	transfected astrocytes	synaptobrevin2 vesicular arrangement
Tharkeshwar, A. K., et al., (2017). A novel approach to analyze lysosomal dysfunctions through subcellular proteomics and lipidomics: the case of NPC1 deficiency. Scientific Reports, 7:41408, doi:10.1038/srep41408	HeLa cells, Superparamagnetic iron oxide nanoparticles (SPIONS)	CLEM with SIM and TEM
Ovciarikova, J., et al., (2017). Mitochondrial behaviour throughout the lytic cycle of Toxoplasma gondii. Scientific Reports, 7:42746, doi:10.1038/srep42746	Parasites grown in human foreskin fibroblasts	mitochondrial morphology and positioning of Toxoplasma gondii
van Vilet, A. R., et al., (2017). The ER Stress Sensor PERK Coordinates ER-Plasma Membrane Contact Site Formation through Interaction with Filamin-A and F-Actin Remodeling. Molecular Cell 65, 1–15 March 2, 2017 Elsevier Inc. doi:10.1016/j.molcel.2017.01.020	cultured cells	Colocalization between the G-actin (DNase I) and F-actin (phalloidin)
Thorpe, S. D., et al., (2017). Reduced primary cilia length and altered Arl13b expression are associated with deregulated chondrocyte hedgehog signalling in alkaptonuria, Journal of Cellular Physiology, February 2, 2017, doi:10.1002/jcp.25839	axoneme primary cilia	Cilia diameter was assessed from Arl13b and acetylated α-tubulin
Kilpatrick, L. E., et al., (2017). Real-time analysis of the binding of fluorescent VEGF165a to VEGFR2 in living cells: Effect of receptor tyrosine kinase inhibitors and fate of internalized agonist-receptor complexes., Biochemical Pharmacology, doi:10.1016/j.bcp.2017.04.006	HEK293T cells	HaloTag VEGFR2 and VEGF-A isoforms colocalization, real time quantitative evaluation of VEGFR2 and binding characteristics in living cells using bioluminescence energy transfer (BRET)
Elsutohy, M. M. M., et al., (2017). Real-time measurement of the intracellular pH of yeast cells during glucose metabolism using ratiometric fluorescent nanosensors. Nanoscale, The Royal Society of Chemistry SN - 2040-3364, 2017, doi:10.1039/C7NR00906B	yeast (Saccharomyces cerevisiae)	glucose metabolism and pH regulation in yeast cells, ratiometric fluorescent pH-sensitive nanosensors
Boedeker, C., et al., (2017). Determining the bacterial cell biology of Planctomycetes. Nat. Commun. 8, 14853 doi:10.1038/ncomms14853	planctomycetes (Planctopirus limnophila, Gemmata obscuriglobus and Rhodopirellula baltica.)	SR-SIM imaging of cytoplasm, nucleoids, membranes of planctomysetes
Pina, F., et al., (2017).The Generation of Compartmentalized Nanoparticles Containing SiRNA and Cisplatin using a Multi-Needle Electrohydrodynamic Strategy. Nanoscale, doi:10.1039/C7NR01002H	nanoparticles loaded with an anticancer agent and siRNA	internal structure of nanoparticles examined by TEM and SR-SIM
Viver, T., et al., (2017). The low diverse gastric microbiome of the jellyfish Cotylorhiza tuberculata is dominated by four novel taxa. Environmental Microbiology, 1462-2920, 2017, doi:10.1111/1462-2920.13763	jellyfish (Cotylorhiza tuberculata)	catalyzed reporter deposition fluorescence in situ hybridization (CARD-FISH)
Demmerle, J., et al., (2017). Strategic and practical guidelines for successful structured illumination microscopy. Nature Protocols 12, 988-1010. doi:10.1038/nprot.2017.019	calibration samples	Protocol for generating high quality SIM data
Liang, H., et al., (2017). Metabolic labelling of the carbohydrate core in bacterial peptidoglycan and its applications. Nature Communications, 8:15015, doi:10.1038/ncomms15015	Bacteria (E. coli and P. putida)	SIM and 3D localization microscopy of N-acetyl-muramic acid backbone of bacterial peptidoglycan labeled with click chemistry
Gray, R. D. M., et al., (2017). Open-source Single-particle Analysis for Superresolution Microscopy with VirusMapper. Jove Issue 122, doi:10.3791/55471	vaccinia virus	SIM imaging used for localization of proteins on virus particles. Development of VirusMapper an ImageJ plugin for single-particle analysis of superresolution images
Markert, S. M., et al., (2017). 3D subcellular localization with superresolution array tomography on ultrathin sections of various species. Methods in Cell Biology, Volume 140, ISSN 0091-679X, doi:10.1016/bs.mcb.2017.03.004	Ultrathin plastic sections of Caenorhabditis elegans, Trypanosoma brucei, and brain tissue of Cataglyphis fortisand Apis mellifera	Correlative Array Tomography using SIM and scanning electron microscopy
Zobel, T., Bogdan, S., (2013). A high resolution view of the fly actin cytoskeleton lacking a functional WAVE complex. Journal of Microscopy, 251: 224–231. doi:10.1111/jmi.12020	Drosophila Schneider (S2R+) cells, and 70 µm thick Drosophila wild-type and abi-mutant egg chambers	SIM imaging of the actin cytoskeleton, membrane dynamics, and 70 µm thick egg chambers

Superresolution Structured Illumination Microscopy (cont.)

Publication	Sample	Application
Söderström, B., et al., (2014). Disassembly of the divisome in Escherichia coli: evidence that FtsZ dissociates before compartmentalization. Molecular Microbiology, 92: 1–9. doi:10.1111/mmi.12534	Escherichia coli	Confocal, FRAP, and SIM imaging of divisome proteins in E. coli.
Westin, L., et al., (2014). Nanoscopic spine localization of Norbin, an mGluR5 accessory protein. BMC Neuroscience, 2014 15:45, doi:10.1186/1471-2202-15-45	Neuronal spines	3D-SIM imaging of Norbin, postsynaptic density protein 95 (PSD-95), actin and mGluR5 in spines
Fukuda, T., et al., (2014). STAG3-mediated stabilization of REC8 cohesin complexes promotes chromosome synapsis during meiosis. The EMBO Journal 33: 1243–1255, doi:10.1002/embj.201387329	spermatocytes	Investigation of in vivo function of STAG3, a vertebrate meiosis-specific SA protein using SIM
Lasič, E., et al., (2017). Dynamin regulates the fusion pore of endo- and exocytotic vesicles as revealed by membrane capacitance measurements, Biochimica et Biophysica Acta (BBA) - General Subjects, Volume 1861, Issue 9, 2017, Pages 2293-2303, ISSN 0304-4165, doi:10.1016/j.bbagen.2017.06.022	cultured rat astrocytes	SIM imaging and capacitance measurements of single vesicles to characterize dynamin regulation of the fusion pore
Dvořáčková, M., et al., (2017). Replication of ribosomal DNA in Arabidopsis occurs both inside and outside the nucleolus during S phase progression, J Cell Sci, doi:10.1242/jcs.202416	Arabidopsis	Determination of the subnuclear distribution of ribosomal DNA during S phase.
Masters, T. A., et al., (2017). MYO6 Regulates Spatial Organization of Signaling Endosomes Driving AKT Activation and Actin Dynamics, Cell Reports, Volume 19, Issue 10, 2017, Pages 2088-2101, ISSN 2211-1247, doi:10.1016/j.celrep.2017.05.048	HeLa cells	SIM imaging of endosomes and actin
Chasen, N. M., et al., (2017). A Glycosylphosphatidylinositol-Anchored Carbonic Anhydrase-Related Protein of Toxoplasma gondii Is Important for Rhoptry Biogenesis and Virulence, mSphere May 2017, 2 (3) e00027-17; doi:10.1128/mSphere.00027-17	Toxoplasma gondii	SIM imaging of carbonic anhydrase-related proteins in tachyzoites
Müller, P., et al., (2017). Intramyocardial fate and effect of iron nanoparticles co-injected with MACS purified stem cell products, Biomaterials, Volume 135, 2017, Pages 74-84, ISSN 0142-9612, doi:10.1016/j.biomaterials.2017.05.002	stem cells	SIM images of cellular location of MACS MicroBeads, clinical application

Further Reading

1. Gustafsson et al., (2008). Three dimensional resolution doubling in wide-field fluorescence microscopy by structured illumination, Biophysical Journal, Volume 94, Issue 12, 4957-4970, doi:10.1529/biophysj.107.120345
2. Betzig et al., (2006). Imaging Intracellular Fluorescent Proteins at Nanometer Resolution, Science 15 Sept 2006: 1642-1645, doi:10.1126/science.1127344
3. Patterson et al., (2010). Superresolution imaging using single-molecule localization, Annu Rev Phys Chem, doi:10.1146/annurev.physchem.012809.103444
4. Baddeley et al., (2011). Three-dimensional sub-100 nm super-resolution imaging of biological samples using a phase ramp in the objective pupil, Nano Res. 4(589), doi:10.1007/s12274-011-0115-z
5. White Paper: Correlative Protein Localization in Yeast. High-Resolution Localization of Fluorescent Proteins Using Shuttle & Find for Superresolution and Scanning Electron Microscopy. For download click here.
6. White Paper: ZEISS ELYRA Sample Preparation for Superresolution Microscopy – a Quick Guide. For download click here.

Carl Zeiss Microscopy GmbH
07745 Jena, Germany
microscopy@zeiss.com
www.zeiss.com/elyra